Ⅲ．研究成果の刊行に関する一覧表

別紙４

研究成果の刊行に関する一覧表

雑誌

発表者氏名	論文タイトル名	発表誌名	巻号	ページ	出版年
Mimuro, J., Mizukami, H., Hishikawa, S., Ikemoto, T., Ishiwata, A., Sakata, A, Ohmori, T., Madoiwa, S., Ono, F., Ozawa, K., and Sakata, Y.	Minimizing the inhibitory effect of neutralizing antibody for efficient gene expression in the liver with adeno-associated virus 8 vectors.	Mol. Ther.	21(2)	318-323	2013
Miyata, S., Urabe, M., Gomi, A., Nagai, M., Yamaguchi, T., Tsukahara, T., Mizukami, H., Kume, A., Ozawa, K., Watanabe, E.	An R132H mutation in isocitrate dehydrogenase 1 enhances p21 expression and inhibits phosphorylation of retinoblastoma protein in glioma cells.	Neurol. Med. Chir. (Tokyo)	53(10)	645-54	2013
Shimada, M., Abe, S., Takahashi, T., Shiozaki, K., Okuda. M., Mizukami. H., Klinman, D.M., Ozawa, K., and Okuda., K.	Prophylaxis and treatment of Alzheimer's disease by delivery of an adeno-associated virus encoding a monoclonal antibody targeting the amyloid protein.	PLoS One	8(3)	e57606	2013
Tsukahara, T., Ohmine, K., Yamamoto, C., Uchibori, R., Ido, H., Teruya, T., Urabe, M., Mizukami, H., Kume, A., Nakamura, M., Mineno, J., Takesako, K., Riviere, I., Sadelain, M., Brentjens, R., Ozawa, K.	CD19 target-engineered T-cells accumulate at tumor lesions in human B-cell lymphoma xenograft mouse models.	Biochem. Biophys. Res. Commun.	438(1)	84-9	2013
Takahashi, K., Mizukami, H., Saga, Y., Takei, Y., Urabe, M., Kume, A., Machida, S., Fujiwara, H., Suzuki, M., Ozawa, K.	Suppression of lymph node and lung metastases of endometrial cancer by muscle-mediated expression of soluble vascular endothelial growth factor receptor-3.	Cancer Sci.	104(8)	1107-11	2013
Uchibori, R., Tsukahara, T., Mizuguchi, H., Saga, Y., Urabe, M., Mizukami, H., Kume, A., and Ozawa, K.	NF-κB activity regulates mesenchymal stem cell accumulation at tumor sites.	Cancer Res.	73(1)	364-372	2013

Kashiwakura, Y., Ohmori, T., Mimuro, J., Madoiwa, S., Inoue, M., Hasegawa, M., Ozawa, K., and Sakata, Y.	Production of functional coagulation factor VIII from iPSCs using a lentiviral vector.	Haemophilia	20	e40-44	2014
Uehara, T., Kanazawa, T., Mizukami, H., Uchibori, R., Tsukahara, T., Urabe, M., Kume, A., Misawa, K., Carey, T. E., Suzuki, M., Ichimura, K., Ozawa, K.	Novel anti-tumor mechanism of galanin receptor type 2 in head and neck squamous cell carcinoma cells.	Cancer Sci.	105(1)	72-80	2014
Koyama D, Kikuchi J, Hiraoka N, Wada T, Kurosawa H, Chiba S, and Furukawa Y	Proteasome inhibitors exert cytotoxicity and increase chemosensitivity via transcriptional repression of Notch1 in T-cell acute lymphoblastic leukemia	Leukemia	epub	doi: 10.1038/leu. 2013.366	2013
Tago K, Funakoshi-Tago M, Itoh H, Furukawa Y, Kikuchi J, Kato T, Suzuki K, and Yanagisawa K	Arf tumor suppressor disrupts the oncogenic positive feedback loop including c-Myc and DDX5.	Oncogene	epub	doi: 10.1038/onc. 2013.561	2014
Kuroda I, Inukai T, Zhang X, Kikuchi J, Furukawa Y, Nemoto A, Akahane K, Hirose K, Honna-Oshiro H, Goi K, Kagami K, Yagita H, Tauchi T, Maeda Y, Sugita K	BCR-ABL regulates death receptor expression for TNF-related apoptosis-inducing ligand (TRAIL) in Philadelphia chromosome-positive leukemia.	Oncogene	32	1670-1681	2013
Kikuchi J, Yamada S, Koyama D, Wada T, Nobuyoshi M, Izumi T, Akutsu M, Kano Y, and Furukawa Y	The novel orally active proteasome inhibitor K-7174 exerts anti-myeloma activity *in vitro* and *in vivo* by down-regulating the expression of class I histone deacetylases.	J. Biol. Chem.	288	25593-25602	2013
Kikuchi J, Shibayama N, Yamada S, Wada T, Nobuyoshi M, Izumi T, Akutsu M, Kano Y, Sugiyama K, Ohki M, Park SY, and Furukawa Y	Homopiperazine derivatives as a novel class of proteasome inhibitors with a unique mode of proteasome binding.	PLoS One	8	e60649	2013

Hiraoka N, Kikuchi J, Koyama D, Uesawa M, Akutsu M, Wada T, Abe M, Mori S, Nakamura Y, Kano Y, and Furukawa Y	Purine analog-like properties of bendamustine underlie rapid activation of DNA damage response and synergic effects with pyrimidine analogues in lymphoid malignancies.	PLoS One	9	e90675	2014
Hiraoka N, Kikuchi J, Koyama D, Wada T, Mori S, Nakamura Y, and Furukawa Y	Alkylating agents induce histone H3K18 hyperacetylation and potentiate HDAC inhibitor-mediated global histone acetylation and cytotoxicity in mantle cell lymphoma.	Blood Cancer J.	3	e169	2013

Ⅳ. 研究成果の刊行物・別冊
（主なもの）

Minimizing the Inhibitory Effect of Neutralizing Antibody for Efficient Gene Expression in the Liver With Adeno-associated Virus 8 Vectors

Jun Mimuro[1], Hiroaki Mizukami[2], Shuji Hishikawa[3], Tomokazu Ikemoto[4], Akira Ishiwata[1], Asuka Sakata[1], Tsukasa Ohmori[1], Seiji Madoiwa[1], Fumiko Ono[5], Keiya Ozawa[2] and Yoichi Sakata[1]

[1]Division of Cell and Molecular Medicine, Center for Molecular Medicine, Jichi Medical University, Tochigi-ken, Japan; [2]Division of Genetic Therapeutics, Center for Molecular Medicine, Jichi Medical University, Tochigi-ken, Japan; [3]Division of Medical Skill Training, Center for Development of Advanced Medical Technology, Jichi Medical University, School of Medicine, Tochigi-ken, Japan; [4]Division of Cardiovascular Medicine, Department of Medicine, Jichi Medical University, School of Medicine, Tochigi-ken, Japan; [5]The Corporation for Production and Research of Laboratory Primates, Tsukuba, Japan

Neutralizing antibodies (NAbs) against adeno-associated viruses (AAVs) are known to interfere with AAV vector-mediated gene transfer by intravascular delivery. Evading the inhibitory effects of antibodies against AAV vectors is necessary for efficient transfer of therapeutic genes clinically. For this purpose, we tested the efficacy of saline flushing in order to avoid contact of vectors with NAbs present in blood. Direct injection of the AAV8 vector carrying the *factor IX* (*FIX*) gene into the portal vein of macaques using saline flushing achieved transgene-derived FIX expression (4.7 ± 2.10–10.1 ± 5.45% of normal human FIX concentration) in the presence of NAbs. Expression was as efficient as that (5.43 ± 2.59–12.68 ± 4.83%) in macaques lacking NAbs. We next tested the efficacy of saline flushing using less invasive balloon catheter-guided injection. This approach also resulted in efficient expression of transgene-derived FIX (2.5 ± 1.06–9.0 ± 2.37%) in the presence of NAbs (14–56× dilutions). NAbs at this range of titers reduced the efficiency of transduction in the macaque liver by 100-fold when the same vector was injected into mesenteric veins without balloon catheters. Our results suggest that portal vein-directed vector delivery strategies with flushing to remove blood are efficacious for minimizing the inhibitory effect of anti-AAV antibodies.

Received 21 August 2012; accepted 14 November 2012; advance online publication 18 December 2012. doi:10.1038/mt.2012.258

INTRODUCTION

Gene and cell therapies are expected to be the next generation of therapies for a variety of inherited diseases. Hemophilia is thought to be an ideal target disease for these approaches as it is caused by a genetic abnormality in the factor VIII gene for hemophilia A, or the factor IX (FIX) gene for hemophilia B.[1–7] The current strategy of hemophilia gene therapy involves inducing expression of the normal coagulation factor gene or transplanting cells expressing the respective coagulation factor. The liver is normally the primary target of gene transfer for coagulation factors since the majority of these coagulation factors are synthesized in the liver with appropriate post-translation modifications before secretion into the circulatory system.

Substantial effort has been applied to express coagulation factor genes using various vector types. Among the viral vectors, recombinant adeno-associated virus (AAV) vectors are preferred for therapeutic gene transfer *in vivo* because they reside in the episome and rarely integrate into genomes. However, retrovirus vectors including lentivirus vectors require integration into the host cell genome.[6,7] In addition, AAV vectors can transfer genes to nondividing cells and allow long-term expression of transgenes in these cells.

Clinical trials for hemophilia gene therapy have recently been conducted using various types of vectors.[4–11] These trials were designed based upon data obtained from mouse models of hemophilia and hemophiliac dogs and proved to be more efficient in these models than for humans. Species differences between humans and these other animal models might partially account for the results observed. Therefore, gene transfer studies in non-\ human primates may well predict the efficacy of gene transfer in humans. Indeed, *FIX* gene transfer studies using a new type of vector have been conducted in rhesus macaques.[12,13] The results from these studies provided the basis for recent hemophilia B gene therapy clinical trials employing an AAV8 vector.[13–16] Gene transfer in mice using AAV vectors results in excellent transduction efficiency. This is especially so for AAV8 vector-mediated gene transfer in the mouse liver;[12–14,17] however, the efficacy of AAV8 vectors is modest in macaques.[13]

There are also difficulties associated with *FIX* gene expression when using AAV8 vectors in nonhuman primates. Growing evidence suggests that the presence of neutralizing antibodies (NAbs) against AAV8, due to previous natural infection by wild-type AAV, significantly inhibits transduction in the macaque liver. It is likely that antibodies against one serotype of AAV cross-react with other AAV serotypes.[18] A hemophilia B gene therapy

J.M., H.M., S.H., and T.I. contributed equally to this work.

Correspondence: *Jun Mimuro, Division of Cell and Molecular Medicine, Center for Molecular Medicine, Jichi Medical University, 3311-1 Yakushiji, Shimotsuke 329-0498, Japan. E-mail: mimuro-j@jichi.ac.jp*

Table 1 Expression of macaque T262A in nonhuman primates with AAV8-HCRHAAT-macFIXT262A

Macaque number	Age	Vector dose (vg/kg)	Route of vector injection	FIX T262A concentration (%)	Vector genome copies in liver tissue (vg/diploid genome)	Anti-AAV8 NAb titer
#14	5.7	1×10^{12}	Mesenteric vein	0.02 ± 0.019	0.1	56×
#17	5.8	1×10^{13}	Mesenteric vein	0.13 ± 0.081	0.4	56×
#24	6.6	1×10^{12}	Mesenteric vein	0.09 ± 0.048	0.5	14×
#28	7.8	5×10^{12}	Saphenous vein	12.68 ± 4.83	38.2	Negative
#30	2.9	5×10^{12}	Saphenous vein	5.43 ± 2.59	48.2	Negative
#31	2.9	5×10^{12}	Saphenous vein	7.64 ± 2.32	49.6	Negative

Abbreviations: AAV, adeno-associated virus; FIX, factor IX; HAAT, α1-antitrypsin; HCR, hepatic control region.
The concentration of macaque FIX T262A is expressed as a percentage of normal human plasma FIX concentration; anti-AAV8 neutralizing antibody (NAb) titer is expressed as the final dilution of the test serum in the assay; vector genome (vg) copies in liver cells were determined by quantitative PCR and expressed as copy numbers per cell.

clinical study using an AAV8 vector was successfully conducted in hemophilia B patients negative for pre-existing antibodies against AAV8.[15] Because of the high prevalence of AAV infection in humans,[18] evading NAbs against this virus is an important hurdle to overcome before AAV8 vectors can be routinely and effectively employed for therapies.

The aim of our study was to develop an administration method of AAV8 vectors that assisted in minimizing the inhibitory effect of NAbs against AAV in macaques that were already seropositive for AAV8 antibodies.

RESULTS

The AAV8 vector carrying the macaque *FIX T262A* gene located downstream of the liver-specific chimeric promoter consisted of an enhancer element of hepatic control region (HCR) of the *ApoE/C-I* gene and the 5′ flanking region of the *α1-antitrypsin* (HAAT) gene (AAV8-HCRHAAT-macFIXT262A). This vector was used to express mutant macaque FIX containing a single amino acid substitution of Thr to Ala at the position 262 (macaque FIX T262A) in the following experiments. Macaque FIX T262A but not wild-type macaque FIX could be bound to human FIX-specific monoclonal antibody 3A6, thereby macaque FIX T262A expressed in macaques with AAV8-HCRHAAT-macFIXT262A could be precisely quantified by an enzyme immunoassay with 3A6.[17] The amino acid sequence of macaque FIX is highly homologous to the human FIX amino acid sequence. Twelve amino acid residues of human FIX are different at corresponding positions of macaque FIX, while only one amino acid of macaque FIX T262A is different from wild-type macaque FIX. Expression of macFIX T262A in a macaque would mimic a situation where normal human FIX is expressed in a hemophilia B patient with a missense mutation in the *FIX* gene.

Results corresponding to the expression of macaque FIX T262A following injection of AAV8HCRHAATmacFIXT262A can be seen in Table 1. When AAV8HCRHAATmacFIXT262A (5×10^{12} vector genome copies (vg)/kg) was injected into the saphenous veins of three AAV8 NAb-negative macaques (#28, #30, #31), expression of macFIX T262A in the therapeutic range (>5% of normal FIX concentration) was achieved. However, injection of the same vector (1×10^{12}–1×10^{13} vg/kg) into the mesenteric vein branches of AAV8 NAb-positive macaques (#14, #17, #24; inhibitory titers: 14–56×) resulted in subtherapeutic levels (<0.2%) of macFIX T262A expression. The amount of vector DNA in the liver of AAV8 NAb-positive macaques was ~1% of that seen in AAV8 NAb-negative macaques (Table 1). These data suggest that low titers of NAbs against AAV8 significantly inhibit transduction even when the vector is injected into the mesenteric vein branches. In addition, only short period of time may be required for NAbs in the blood to neutralize the AAV8 vector since the blood of the mesenteric vein rapidly goes to the liver through the portal vein after gathering with the blood from other viscera.

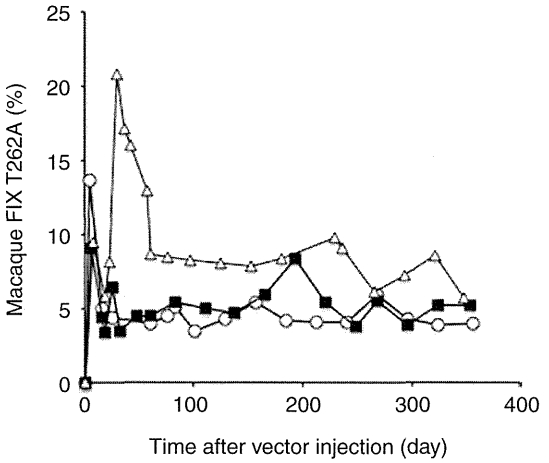

Figure 1 Expression of FIX T262A in macaques after direct vector injection into portal veins. Macaques (n = 3) were subjected to direct injection of AAV8 vector into the portal vein. Concentrations of FIX T262A in macaque plasma samples (macaque #26, open triangles; #27, open circles; #29, closed squares) were measured by ELISA. AAV, adeno-associated virus; ELISA, enzyme-linked immunosorbent assay; FIX, factor IX.

Evading AAV8 NAbs could be achieved by ensuring the AAV8 vector and NAbs do not come into physical contact with each other in the blood. Blood enters the liver from the hepatic artery and portal vein. The hepatic artery accounts for ~20–30% of blood flow, while the portal vein supplies the remaining blood flow to hepatocytes.[19,20] Blood from the portal vein and hepatic artery are eventually mixed in the sinusoids of the liver; however, the blood from the portal vein mainly supplies hepatocytes. Therefore, direct injection of AAV8 vectors into the portal vein branch was

Table 2 Expression of macaque T262A in nonhuman primates with direct, and balloon catheter-guided vector (AAV8-HCRHAAT-macFIXT262A) injection into the portal vein

Macaque ID	Age	Vector dose (vg/kg)	Injection method to portal vein branch	FIX T262A concentration (%)	Vector genome copies in liver tissue (vg/diploid genome)	Anti-AAV8 NAb titer
#26	10.1	5×10^{12}	Direct	4.7 ± 2.10	77.9	28×
#27	7.4	5×10^{12}	Direct	10.1 ± 5.45	28.5	14×
#29	11.0	5×10^{12}	Direct	5.3 ± 1.40	64.3	14×
#37	7.5	5×10^{12}	Catheter-guided	9.0 ± 2.37	61.1	14×
#38	10.7	5×10^{12}	Catheter-guided	3.2 ± 1.21	13	56×
#42	7.7	5×10^{12}	Catheter-guided	2.5 ± 1.06	15.3	14×

Abbreviations: AAV, adeno-associated virus; FIX, factor IX; HAAT, α1-antitrypsin; HCR, hepatic control region; Nab, neutralizing antibody.
FIX T262A concentration is expressed as a percentage of normal human plasma FIX concentration; anti-AAV8 NAb titer is expressed as the final dilution of the test serum in the assay; vector genome (vg) copies in liver cells were determined by quantitative PCR and expressed as copy numbers per cell.

investigated to determine whether saline flushing to remove blood from the portal vein just before injection of the vector would diminish the inhibitory effects of anti-AAV8 NAbs. Three macaques (#26, #27, #29; inhibitory titers: 14–28×) were directly injected with vector (5×10^{12} vg/kg) into the left portal vein after flushing saline to remove blood (**Supplementary Table S1**). Expression of transgene-derived FIX (macaque FIX T262A) increased to therapeutic levels with the AAV8 vector carrying the macaque *FIX T262A* gene and persisted for greater than 1 year in the three macaques (Figure 1). Average FIX and vector genome levels in macaque liver tissues are presented in Table 2. Compared with the results of vector injection to the mesenteric vein of NAb-positive macaques #14, #17, and #24 (Table 1), the levels of macaque FIX T262A in the circulation of the macaques #26, #27, and #29 that received vector injection directly to the left portal vein with flushing to remove blood, were increased to therapeutic levels with significant amounts of vector genome detected (Table 2).

Blood chemistry analysis and liver biopsies were conducted following administration of the vector to determine whether there were any adverse effects induced by the injection. Moderate increases in liver enzymes, such as transaminases, were observed just after injection of the vector (**Supplementary Figure S1**). However, no significant pathological changes were seen in liver biopsy samples taken on days 14, 28 or 48 (data not shown). We did not observe an increase in the number of TUNEL (terminal deoxynucleotidyl transferase-mediated dUTP nick-end labeling)-positive hepatocytes in the liver biopsy specimens (data not shown).

The direct injection of the AAV8 vector into the left portal vein branch with saline flushing to remove blood from the portal vein just before injection of the vector was effective to minimize the inhibitory effects of anti-AAV8 NAbs. Therefore, we explored the possibility of utilizing a balloon catheter to perform the vector injection into the portal vein branch with saline flushing to remove blood, taking the concern about the safety of the procedures into consideration. Using a microballoon catheter, we injected the vector into the left portal vein of three anti-AAV8 antibody-positive macaques (#37, # 38, #42; inhibitory titers: 14–56×) (Table 2, **Supplementary Table S2**). Fluorography in macaque #37 representing angiography of the portal vein branch is shown in Figure 2 and **Supplementary Video S1**. Increase of FIX T262A to therapeutic levels was achieved in the three macaques (#37, # 38, #42),

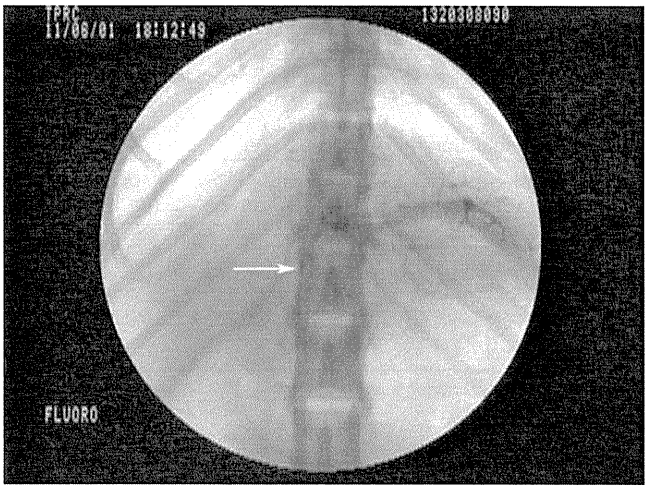

Figure 2 Fluorography in macaque #37. A balloon catheter was inserted into the portal vein of macaque #37 and contrast medium injected before vector administration. The left portal vein branches can be visualized. The arrow (white) indicates the tip of the catheter. See **Supplementary Video S1** which also recorded inflation of the balloon before the vector administration and deflation of the balloon after the administration.

and macaque FIX T262A expression in the circulation persisted (Figure 3, Table 2). The two portal vein vector delivery methods were successful in expressing macaque FIX T262A with the AAV8 vector in NAb-positive macaques (Table 2). The data suggest that the gene transfer efficiency using the catheter-guided vector injection method is similar to that of the direct vector injection into the portal vein branch with flushing.

Blood chemistry analysis and liver biopsies were conducted following injection of the vector. Increases in the levels of liver enzymes just after injection of the vector were not observed, suggesting that the ischemic effect of the temporary occlusion of the left portal vein branch was minimum compared with that of the direct vector injection procedure. Moderate increases in transaminases were observed following the vector injection, but did not persist (**Supplementary Figure S1**). Although the cause of the changes in the liver enzymes was not elucidated, no animals showed pathological changes, including histology of liver biopsy samples (data not shown).

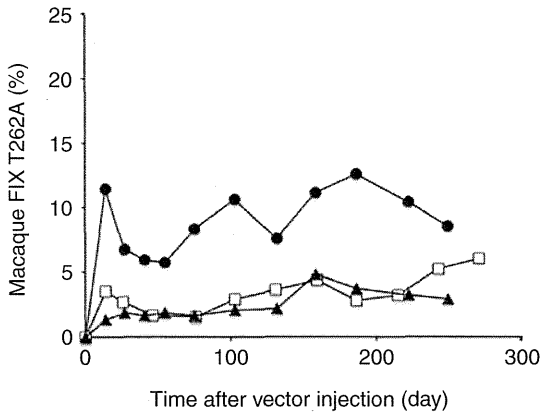

Figure 3 Expression of FIX T262A in macaques following balloon catheter-guided vector injection into portal veins. Three macaques (n = 3) were subjected to balloon catheter-guided vector injection into the portal vein. Concentrations of FIX T262A in macaque plasma samples (#37, closed circles; #38, open squares; #42, closed triangles) were measured by ELISA. ELISA, enzyme-linked immunosorbent assay; FIX, factor IX.

Table 3 Vector injection rate

Route of injection (macaque number)	Elapsed time (seconds)	Rate of injection (vg/kg/second)
Mesenteric vein (#14, #17, #24)	5	2×10^{11}–2×10^{12}
Saphenous vein (#28, #30, #31)	5	1×10^{12}
Portal vein (direct) (#26, #27, #29)	8–10	5×10^{11}
Portal vein (catheter) (#37, #38, #42)	15–22	2.3×10^{11}–3.3×10^{11}

Abbreviation: vg, vector genome.

Vector injection rates of the four different vector injection procedures are listed in Table 3 for comparison. The vector injection rates of the portal vein-directed strategies were similar to those of bolus vector injection into the saphenous vein and the mesenteric vein. Thus, the effect of vector injection speed on the transduction efficiency of the vector was thought to be minimal.

DISCUSSION

There are many features that make recombinant AAV vectors attractive for transferring therapeutic genes into target organs, and many vectors have been tried for the treatment of various diseases.[6,7,11,15,21–23] However, lines of evidence suggest that NAbs against AAV interfere with AAV vector-mediated gene transfer by intravascular vector delivery.[7,23–26] A clinical gene therapy trial for hemophilia B using a self-complementary AAV8 vector carrying the FIX gene has been conducted and reported to be successful.[15] However, even the self-complementary AAV8 vector failed to express FIX in a subject with a relatively high anti-AAV8 antibody titer compared with other subjects with no or lower antibody titers.[15]

According to the previous reports on the prevalence of NAbs against various AAV serotypes in normal subjects, the seropositivity against AAV8 is 15–30%, which is lower than that against AAV2 (50–60%), although the technical details of the NAb assay is different.[27,28] These reports have also demonstrated that the antibody titer against AAV8 is generally lower than for AAV2. Our data suggest that a low titer of NAbs against AAV8 can interfere with transduction even if the vector is injected into the mesenteric vein. Therefore, the use of another serotype vector such as AAV5 vector could be the next approach for this type of gene therapy because of the divergence in capsid sequence of AAV5 from other AAV serotypes.[13,16] Although the prevalence of NAbs against AAV5 is much lower than those against AAV1 and AAV2, and the prevalence of NAbs against AAV5 is comparable to or even lower than that against AAV8 in humans,[25,27] it is possible that subjects of gene therapy may contain cross-reactive NAbs against various AAV serotypes.

Another approach for evading NAbs against AAV could be the use of chemically or genetically modified AAV variants. Such variants could include AAV vector mutants with amino acid substitutions, or chimeric AAV vectors made by serotype shuffling.[23] Approaches that enable evasion of NAb inhibitory effects are necessary if researchers and clinicians wish to effectively apply AAV vectors for gene therapy because of NAb cross-reactivity.

An alternative approach for overcoming the inhibitory effect of NAb against AAVs is to develop a vector injection method. In the current study, two portal vein vector delivery strategies were employed that ensured that the AAV8 vector and NAbs do not come into physical contact with each other in the blood. These strategies were investigated using macaques whether the strategies could efficiently transduce hepatocytes with the AAV8 vector in the presence of NAbs. The first approach was the direct injection of AAV8 vectors into the portal vein branch after flushing with saline to remove blood. This strategy proved to be successful for the vector expressing FIX T262A in anti-AAV8 antibody-positive macaques. Since there are safety concerns about the direct vector injection method, injection of the vector into the portal vein using a balloon catheter was investigated. The catheter-guided vector injection may be less invasive than the direct vector injection into the portal vein branch because exfoliation of hepatic hilum is not required. In addition, fine surgical skills, such as manipulation of the hepatic hilum and suturing the venotomy site of portal vein after the direct vector injection without causing stenosis, are required for the direct vector injection method into the left portal vein. Obviously, catheterization from the mesenteric vein branch is required for the balloon catheter-guided vector injection method but insertion of a catheter into the portal vein from a branch of the mesenteric vein is not difficult for a cardiologist and a radiologist familiar with angiography. In addition, suturing the venotomy site of the mesenteric vein branch is easier and safer than suturing the venotomy site of portal vein, and the ischemic effect of this procedure was expected to be less than that of the direct vector injection into the portal vein branch. Taken together, these studies suggested that both the direct vector injection into the left portal vein and the balloon catheter-guided vector injection into the left portal vein were similarly effective for hepatocyte transduction with the AAV8 vector in the presence of low titer NAbs but the balloon catheter-guided vector injection method into the left portal vein was thought to be safer than the direct vector injection into the left portal vein.

Considering that the antibody titer against AAV8 was generally lower than that against AAV2 and that NAbs at low titers could interfere with the AAV8 vector-mediated gene transfer to the liver significantly, we selected macaques with low NAb titers

for the portal vein vector delivery strategies. However, the impact of the presence of high titer NAbs on the efficacy of these methods was not studied. Thus, the extent of AAV8 NAb titer, for that this approach is effective, needs to be investigated in the future.

In conclusion, we have provided the basis for an alternative approach for gene transfer to the liver that minimizes the deleterious effects of anti-AAV NAbs. Our result might expand the potential of the AAV vector-mediated gene delivery for medical application.

MATERIALS AND METHODS

AAV vector production. Construction of pAAV2-HCRHAAT-macFIX T262A and production of AAV8 carrying the macaque FIX T262A gene (AAV8HCRHAATmacFIXT262A) has been previously described.[17] Briefly, DNA fragments harboring the *macFIXT262A* gene located downstream of the chimeric promoter consisted of an enhancer element of HCR of the human ApoE/C-I gene and the 5′ flanking region of the human HAAT gene (HCRHAAT promoter), and the SV40 polyadenylation signal sequence flanked by AAV2 inverted terminal repeats in pAAV2-HCRHAAT-macFIX T262A. The genes were packaged by triple plasmid transfection of human embryonic kidney 293 cells (Avigen, San Diego, CA) to generate AAV8-HCRHAAT-macFIXT262A, with the chimeric packaging plasmid (AAV2 rep/AAV8 cap), and the adenovirus helper plasmid pHelper (Stratagene, La Jolla, CA), as previously described.[17] The chimeric packaging plasmid for AAV8 capsid pseudotyping[29] was constructed by inserting the synthetic AAV8 *Cap* gene (Takara Bio, Otsu, Shiga, Japan) downstream of the AAV2 Rep gene of pHelp19. For virus vector purification, the DNase (Benzonase; Merck Japan, Tokyo, Japan)-treated viral particles containing samples were subjected to two rounds of cesium chloride-density gradient ultracentrifugation in HEPES-buffered saline (pH 7.4) supplemented with 25 mmol/l EDTA at 21 °C, as previously described.[17] Titration of recombinant AAV vectors was carried out by quantitative PCR using a real-time PCR system (StepOnePlus; Applied Biosystems Japan, Tokyo, Japan).[17] AAV8HCRHAATmacFIXT262A was previously shown to express macaque FIXT262A in mice efficiently.[17] Human FIX could be expressed in macaques and detected, however, macaques developed antibody against human FIX under certain experimental conditions. Only one amino acid residue at position 262 was humanized in macaque FIX T262A for detection with the human FIX-specific monoclonal antibody.

Animals. Cynomolgus macaques were bred and maintained at the Tsukuba Primate Research Center (Ibaraki, Japan). The animal experiments using macaques were performed at the Tsukuba Primate Research Center according to the guidelines of the Institutional Animal Care and Concern Committees at Jichi Medical University and the Tsukuba Primate Research Center. The use of macaques in animal experiments was approved by the Animal Care and Concern Committees. All surgical procedures were carried out under anesthesia, with vital signs and electrocardiogram monitoring conducted in accordance with the stipulated guidelines. Male macaques with low NAb titers (<56×) were used in this study.

Vector injection from peripheral and mesenteric vein. Injection of AAV8 vector to a saphenous vein (peripheral vein) was performed under intramuscular anesthesia. Injection of the AAV8 vector into a terminal branch of the superior mesenteric vein was carried out with laparotomy under anesthesia with isoflurane and electrocardiogram monitoring.

Direct portal vein vector injection with saline flushing. Direct injection of the vector solution into the left portal vein was carried out after induction of general anesthesia with isoflurane and sterilization. A right subcostal incision (5 cm) was made through the skin and the subcutaneous tissue. The abdominal cavity was explored and the soft tissue of hepatic hilum was exfoliated surgically, then the main portal vein and its right and left branches were exposed. The main portal vein was cannulated with a plastic cannula type 20G needle (Surflo; Terumo, Tokyo, Japan), which was advanced into the left portal vein branch. The left and right portal vein branches were then clamped with vascular forceps. After flushing the left portal vein with saline, the vector solution was injected, and then a second saline solution, for flushing, was injected. Volumes of solutions used in the experiments were determined by taking a standard liver volume, a hepatic vascular bed volume, and effects of solutions on the systemic circulation into consideration.[19,30] A standard liver volume of a macaque was estimated with the formula (standard liver volume = 706.2 × body surface area + 2.4)[31] and the vascular bed volume of the liver was estimated to 25–30% of the standard liver volume.[19] A hepatic vascular bed volume can increase to 60% of the liver volume upon infusion of solutions and this may function as a reservoir and reduce the effects of the solutions on the systemic circulation.[20,32,33] The forceps were then removed immediately and the venotomy site was closed with an 8-0 prolene suture.

Catheter-guided vector injection to the portal vein with saline flushing. Balloon catheter-guided injection of the vector into the left portal vein of AAV8 antibody-positive macaques was carried out after the induction of general anesthesia. A 5-cm right paramedian incision was made through the skin and subcutaneous tissue. The abdominal cavity was carefully entered, with a part of the ileum identified and brought out through the incision. A peripheral branch of the superior mesenteric vein was cannulated with a plastic cannula type 20G needle (Surflo; Terumo). A temporary occlusion microcatheter (Iiguman 3.3F; Fuji System, Tokyo, Japan) was advanced into the left portal vein using a guide-wire (run through 0.014 (0.36 mm); Terumo) under a fluoroscope. The positions of the catheter and the balloon were confirmed by imaging with contrast medium. Blood flow in the left portal vein was occluded with a silicone balloon catheter and 40 ml of saline, followed by the AAV8 vector solution, and another 20 ml of saline was injected sequentially through the microcatheter. Volumes of solutions used in the experiments were determined as above with taking the result of the experiment of direct vector injection to the left portal vein branch into consideration. Following deflation of the balloon, the microcatheter was withdrawn and the peripheral venotomy ligated. The abdominal wall was then closed in layers.

Analysis of macaque FIX T262A expression in macaques. Macaque FIX T262A was bound to 3A6, a human FIX-specific monoclonal antibody for analyses. An enzyme-linked immunosorbent assay (ELISA) for the detection of macaque FIX T262A was carried out using 3A6, as previously described.[17,34]

NAb assay. An assay for the detection of anti-AAV8 NAbs was performed as previously reported, with some modifications.[35,36] Briefly, 5×10^4 2V6.11 cells/well were seeded in the wells of 96-well culture plates. Ponasterone A was added to the culture media the day before transduction to induce expression of the E4 gene. On the day of transduction, 10 µl of serum (undiluted, or subject to serial twofold dilutions) was incubated with the vector (AAV8-CMV-LacZ, 5×10^7 vg/10 µl) at 37 °C for 1 hour, and this mixture was added to a culture well. Sucrose was added to the culture medium such that the final concentration was 125 mmol/l. The culture medium was removed after a 48-hour incubation, and β-galactosidase activity quantified with a β-Gal assay kit (Invitrogen, Carlsbad, CA). Briefly, o-nitrophenyl-β-D-galactopyranoside was added to cell lysates, incubated for 30 minutes, and color change quantified with a microplate reader (Benchmark Plus; Bio-Rad, Hercules, CA). If β-galactosidase activity was inhibited with a test sample that contained more than 50% of control fetal bovine serum, it was judged as positive for neutralizing capacity. The inhibitory titer of the serum sample was expressed as the highest final dilution in the culture medium that showed inhibitory activity.

Quantitation of AAV8 vector DNA in macaque tissue. Quantitation of AAV8 vector DNA in macaque tissues was performed using quantitative

PCR assays using a StepOnePlus instrument (Applied Biosystems Japan). DNA was isolated from macaque tissues using a DNeasy Blood & Tissue Kit (QIAGEN, Valencia, CA) and subjected to PCR using primers 5′-GAT AAC TGG GGT GAC CTT GG-3′ and 5′-GCC TGG TGA TTC TGC CAT GA-3′, and Cybergreen reagent (Applied Biosystems Japan).

SUPPLEMENTARY MATERIAL

Figure S1. Changes in aspartate aminotransferase (AST) and alanine aminotransferase (ALT) levels in macaques.
Table S1. Direct vector injection into the portal vein of macaques.
Table S2. Balloon catheter-guided vector injection into macaques.
Video S1.

ACKNOWLEDGMENTS

This study was supported by Grants-in-Aid for Scientific Research (20591155, 21591249, and 21790920) and the Support Program for Strategic Research Infrastructure from the Japanese Ministry of Education, Culture, Sports, Science and Technology; and Health, Labor, and Science Research Grants for Research on HIV/AIDS and Research on Intractable Diseases from the Japanese Ministry of Health, Labor, and Welfare. This work was done in Shimotsuke, Tochigi and Tsukuba, Ibaraki, Japan. The authors declared no conflict of interest.

REFERENCES

1. Mannucci, PM and Tuddenham, EG (2001). The hemophilias–from royal genes to gene therapy. *N Engl J Med* **344**: 1773–1779.
2. Pasi, KJ (2001). Gene therapy for haemophilia. *Br J Haematol* **115**: 744–757.
3. VandenDriessche, T, Collen, D and Chuah, MK (2003). Gene therapy for the hemophilias. *J Thromb Haemost* **1**: 1550–1558.
4. Chuah, MK, Collen, D and Vandendriessche, T (2004). Preclinical and clinical gene therapy for haemophilia. *Haemophilia* **10** (suppl. 4): 119–125.
5. Chuah, MK, Collen, D and VandenDriessche, T (2004). Clinical gene transfer studies for hemophilia A. *Semin Thromb Hemost* **30**: 249–256.
6. Hasbrouck, NC and High, KA (2008). AAV-mediated gene transfer for the treatment of hemophilia B: problems and prospects. *Gene Ther* **15**: 870–875.
7. Mingozzi, F and High, KA (2011). Immune responses to AAV in clinical trials. *Curr Gene Ther* **11**: 321–330.
8. Kay, MA, Manno, CS, Ragni, MV, Larson, PJ, Couto, LB, McClelland, A *et al.* (2000). Evidence for gene transfer and expression of factor IX in haemophilia B patients treated with an AAV vector. *Nat Genet* **24**: 257–261.
9. Jiang, H, Pierce, GF, Ozelo, MC, de Paula, EV, Vargas, JA, Smith, P *et al.* (2006). Evidence of multiyear factor IX expression by AAV-mediated gene transfer to skeletal muscle in an individual with severe hemophilia B. *Mol Ther* **14**: 452–455.
10. Manno, CS, Chew, AJ, Hutchison, S, Larson, PJ, Herzog, RW, Arruda, VR *et al.* (2003). AAV-mediated factor IX gene transfer to skeletal muscle in patients with severe hemophilia B. *Blood* **101**: 2963–2972.
11. Manno, CS, Pierce, GF, Arruda, VR, Glader, B, Ragni, M, Rasko, JJ *et al.* (2006). Successful transduction of liver in hemophilia by AAV-Factor IX and limitations imposed by the host immune response. *Nat Med* **12**: 342–347.
12. Nathwani, AC, Davidoff, AM, Hanawa, H, Hu, Y, Hoffer, FA, Nikanorov, A *et al.* (2002). Sustained high-level expression of human factor IX (hFIX) after liver-targeted delivery of recombinant adeno-associated virus encoding the hFIX gene in rhesus macaques. *Blood* **100**: 1662–1669.
13. Nathwani, AC, Gray, JT, Ng, CY, Zhou, J, Spence, Y, Waddington, SN *et al.* (2006). Self-complementary adeno-associated virus vectors containing a novel liver-specific human factor IX expression cassette enable highly efficient transduction of murine and nonhuman primate liver. *Blood* **107**: 2653–2661.
14. Nathwani, AC, Gray, JT, McIntosh, J, Ng, CY, Zhou, J, Spence, Y *et al.* (2007). Safe and efficient transduction of the liver after peripheral vein infusion of self-complementary AAV vector results in stable therapeutic expression of human FIX in nonhuman primates. *Blood* **109**: 1414–1421.
15. Nathwani, AC, Tuddenham, EG, Rangarajan, S, Rosales, C, McIntosh, J, Linch, DC *et al.* (2011). Adenovirus-associated virus vector-mediated gene transfer in hemophilia B. *N Engl J Med* **365**: 2357–2365.
16. Nathwani, AC, Rosales, C, McIntosh, J, Rastegarlari, G, Nathwani, D, Raj, D *et al.* (2011). Long-term safety and efficacy following systemic administration of a self-complementary AAV vector encoding human FIX pseudotyped with serotype 5 and 8 capsid proteins. *Mol Ther* **19**: 876–885.
17. Ishiwata, A, Mimuro, J, Mizukami, H, Kashiwakura, Y, Yasumoto, A, Sakata, A *et al.* (2010). Mutant macaque factor IX T262A: a tool for hemophilia B gene therapy studies in macaques. *Thromb Res* **125**: 533–537.
18. Calcedo, R, Vandenberghe, LH, Gao, G, Lin, J and Wilson, JM (2009). Worldwide epidemiology of neutralizing antibodies to adeno-associated viruses. *J Infect Dis* **199**: 381–390.
19. Lautt, WW and Greenway, CV (1987). Conceptual review of the hepatic vascular bed. *Hepatology* **7**: 952–963.
20. Saxena R, Zucker SD and Crawford JM (2003). Anatomy and physilogy of the liver. In: Zakim D and Boyer TD (eds). *Hepatology: A Textbook of Liver Disease*, 3rd edn. Saunders: Philadelphia. pp. 3–30.
21. High, KA (2007). Update on progress and hurdles in novel genetic therapies for hemophilia. *Hematology Am Soc Hematol Educ Program*: 466–472.
22. Sands, MS (2011). AAV-mediated liver-directed gene therapy. *Methods Mol Biol* **807**: 141–157.
23. Bartel, M, Schaffer, D and Büning, H (2011). Enhancing the Clinical Potential of AAV Vectors by Capsid Engineering to Evade Pre-Existing Immunity. *Front Microbiol* **2**: 204.
24. Hurlbut, GD, Ziegler, RJ, Nietupski, JB, Foley, JW, Woodworth, LA, Meyers, E *et al.* (2010). Preexisting immunity and low expression in primates highlight translational challenges for liver-directed AAV8-mediated gene therapy. *Mol Ther* **18**: 1983–1994.
25. Li C, Narkbunnam, N, Samulski, RJ, Asokan, A, Hu, G, Jacobson, LJ *et al.* (2012). Neutralizing antibodies against adeno-associated virus examined prospectively in pediatric patients with hemophilia. *Gene Ther* **19**: 288–294.
26. Chandler, RJ and Venditti, CP (2011). A barrel of monkeys: scAAV8 gene therapy for hemophilia in nonhuman primates. *Mol Ther* **19**: 826–827.
27. Boutin, S, Monteilhet, V, Veron, P, Leborgne, C, Benveniste, O, Montus, MF *et al.* (2010). Prevalence of serum IgG and neutralizing factors against adeno-associated virus (AAV) types 1, 2, 5, 6, 8, and 9 in the healthy population: implications for gene therapy using AAV vectors. *Hum Gene Ther* **21**: 704–712.
28. Calcedo, R, Morizono, H, Wang, L, McCarter, R, He, J, Jones, D *et al.* (2011). Adeno-associated virus antibody profiles in newborns, children, and adolescents. *Clin Vaccine Immunol* **18**: 1586–1588.
29. Gao, GP, Alvira, MR, Wang, L, Calcedo, R, Johnston, J and Wilson, JM (2002). Novel adeno-associated viruses from rhesus monkeys as vectors for human gene therapy. *Proc Natl Acad Sci USA* **99**: 11854–11859.
30. Muir, AL, Flenley, DC, Kirby, BJ, Sudlow, MF, Guyatt, AR and Brash, HM (1975). Cardiorespiratory effects of rapid saline infusion in normal man. *J Appl Physiol* **38**: 786–775.
31. Urata, K, Kawasaki, S, Matsunami, H, Hashikura, Y, Ikegami, T, Ishizone, S *et al.* (1995). Calculation of child and adult standard liver volume for liver transplantation. *Hepatology* **21**: 1317–1321.
32. Greenway, CV and Lister, GE (1974). Capacitance effects and blood reservoir function in the splanchnic vascular bed during non-hypotensive haemorrhage and blood volume expansion in anaesthetized cats. *J Physiol (Lond)* **237**: 279–294.
33. Lautt, WW and Greenway, CV (1976). Hepatic venous compliance and role of liver as a blood reservoir. *Am J Physiol* **231**: 292–295.
34. Mimuro, J, Mizukami, H, Ono, F, Madoiwa, S, Terao, K, Yoshioka, A *et al.* (2004). Specific detection of human coagulation factor IX in cynomolgus macaques. *J Thromb Haemost* **2**: 275–280.
35. Moskalenko, M, Chen, L, van Roey, M, Donahue, BA, Snyder, RO, McArthur, JG *et al.* (2000). Epitope mapping of human anti-adeno-associated virus type 2 neutralizing antibodies: implications for gene therapy and virus structure. *J Virol* **74**: 1761–1766.
36. Mohammadi, ES, Ketner, EA, Johns, DC and Ketner, G (2004). Expression of the adenovirus E4 34k oncoprotein inhibits repair of double strand breaks in the cellular genome of a 293-based inducible cell line. *Nucleic Acids Res* **32**: 2652–2659.

ORIGINAL ARTICLE doi: 10.2176/nmc.oa2012-0409

Neurol Med Chir (Tokyo) 53, 645–654, 2013

An R132H Mutation in Isocitrate Dehydrogenase 1 Enhances p21 Expression and Inhibits Phosphorylation of Retinoblastoma Protein in Glioma Cells

Satsuki MIYATA,[1,2] Masashi URABE,[2] Akira GOMI,[3] Mutsumi NAGAI,[1] Takashi YAMAGUCHI,[1] Tomonori TSUKAHARA,[2] Hiroaki MIZUKAMI,[2] Akihiro KUME,[2] Keiya OZAWA,[2] and Eiju WATANABE[1]

[1]Department of Neurosurgery, [2]Division of Genetic Therapeutics, Center for Molecular Medicine, and [3]Department of Pediatric Neurosurgery, Jichi Children's Medical Center, Jichi Medical University, Shimotsuke, Tochigi

Abstract

Cytosolic isocitrate dehydrogenase 1 (IDH1) with an R132H mutation in brain tumors loses its enzymatic activity for catalyzing isocitrate to α-ketoglutarate (α-KG) and acquires new activity whereby it converts α-KG to 2-hydroxyglutarate. The IDH1 mutation induces down-regulation of tricarboxylic acid cycle intermediates and up-regulation of lipid metabolism. Sterol regulatory element-binding proteins (SREBPs) regulate not only the synthesis of cholesterol and fatty acids but also acyclin-dependent kinase inhibitor p21 that halts the cell cycle at G1. Here we show that SREBPs were up-regulated in U87 human glioblastoma cells transfected with an $IDH1^{R132H}$-expression plasmid. Small interfering ribonucleic acid (siRNA) for SREBP1 specifically decreased p21 messenger RNA (mRNA) levels independent of the p53 pathway. In $IDH1^{R132H}$-expressing U87 cells, phosphorylation of Retinoblastoma (Rb) protein also decreased. We propose that metabolic changes induced by the IDH1 mutation enhance p21 expression via SREBP1 and inhibit phosphorylation of Rb, which slows progressionof the cell cycle and may be associated with non-aggressive features of gliomas with an IDH1 mutation.

Key words: isocitrate dehydrogenase 1 (IDH1) mutation, sterol regulatory element-binding proteins (SREBP), p21, lipid metabolism, tricarboxylic acid (TCA) cycle

Introduction

Malignant gliomas are the most frequent and lethal cancers originating in the central nervous system. The most biologically aggressive subtype is glioblastoma (World Health Organization Grade IV). The current standard therapy for glioblastoma is surgical resection followed by adjuvant radiation therapy and administration of an alkylating agent temozolomide, and produces a median survival of only 14.6 months.[21]

Genomic analysis of gliomas has identified mutations in the isocitrate dehydrogenase 1 and 2 (IDH1 and IDH2) genes.[16,25] IDH1 and IDH2 convert isocitrate to α-ketoglutarate (α-KG) producing nicotinamide adenine dinucleotide phosphate. A mutation affecting codon 132 of the IDH1 gene, located on chromosome 2q22, has been found in 12% of glioblastomas,[16] resulting in an Arg to His substitution. Notably, IDH mutations are detected in 95% of secondary gliomas (diffuse astrocytoma, oligodendroglioma, oligoastrocytoma, anaplastic astrocytoma, anaplastic oligodendroglioma, and anaplastic oligoastrocytoma.[25] The presence of the IDH1 mutation has been shown to be associated with a significantly better prognosis (IDH1 mutation versus wild IDH1; 31 months versus 15 months).

$IDH1^{R132H}$ shows decreased enzymatic activity for isocitrate, leading to lower α-KG production. However, it has an altered enzymatic activity and uses α-KG as a substrate to synthesize 2-hydroxyglutarate (2-HG).[6,9,10,26,27] It has been purposed that 2-HG can competitively inhibit α-keto acid transaminase.[18] In addition, levels of tricarboxylic acid (TCA) cycle intermediates were down-regulated and lipid metabolism was up-regulated in mutant IDH1-expressing cells. The IDH mutation has also

Received November 22, 2012; Accepted January 31, 2013

been related to the methylation status of CpG sites, in particular hypermethylation of the methyl guanine methyl transferase (MGMT) promoter.[3,19] Although the mechanism for a favorable prognosis in IDH^{R132H} gliomas has not been fully elucidated, these altered metabolism and methylation statuses are thought to be associated with nonaggressive features.

The sterol regulatory element-binding protein (SREBP) family of transcription factors controls lipid metabolism. SREBP1 consists of SREBP1a and SREBP1c.[7] SREBP1a and SREBP1c are alternate transcripts from a single gene that differ in the first exon.[20] SREBP1c controls the expression of enzymes involved in the synthesis of fatty acids and triglycerides in lipogenic organs. Meanwhile, SREBP1a is highly expressed in cells, which enhances a wide range of enzymes for the synthesis of fatty acids, cholesterol, and phospholipids. SREBP2 regulates cholesterol synthesis. Interestingly, cyclin-dependent kinase inhibitor p21, which halts the cell cycle at the G1 stage, is regulated by SREBP. SREBP1a activates the p21 promoter as strongly as p53, a tumor suppressor positively regulating p21. Increased expression of SREBP1a activates p21 expression, resulting in cell growth arrest.[12]

In the present study, we explore the association between the IDH1 mutation and p21 activation via SREBP and propose a mechanism for a nonaggressive profile in gliomas bearing the IDH1 mutation.

Materials and Methods

I. Plasmids

cDNA of human IDH1 (NM_005896) was purchased from OriGene Technologies (Rockville, Maryland, USA). Site-directed mutagenesis was performed using the KOD-Plus-Mutagenesis Kit (Toyobo, Tokyo) to change G395 to A in IDH1, resulting in an R132H mutation. Wild-type and IDH1^{R132H} cDNAs were excised by EcoRI and EcoRV. The resulting cDNA fragments were cloned into the EcoRI–SmaI sites of pIRES2-EGFP (Addgene, Cambridge, Massachusetts, USA) (Fig. 1A).

II. Cell culture, transfection

U87 cells, a cell line established from glioblastoma, harbor the normal IDH1 gene and the wild-type p53 gene.[23] U87 cells were cultured in Dulbecco's modified Eagle's medium (Invitrogen, Carlsbad, California, USA) with 10% fetal bovine serum. Plasmid transfection was performed with Lipofectamine 2000 (Invitrogen) according to the manufacturer's instructions. Transfection efficiency is reproducibly about 40%, as estimated by counting EGFP-positive

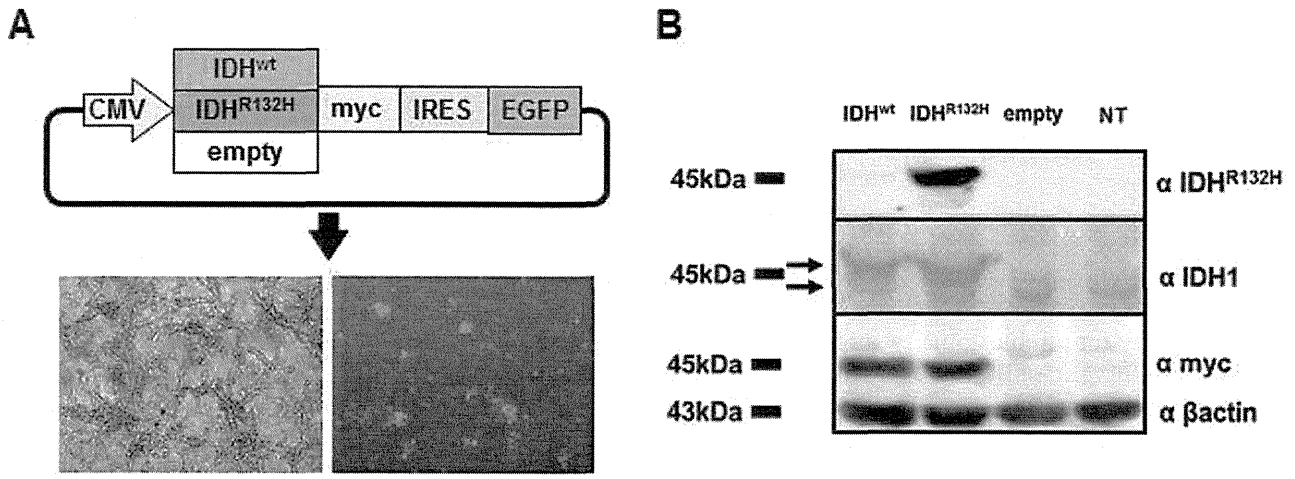

Fig. 1 A: Construction of plasmids and transfection. An R132H mutation in IDH1 was made by converting guanine at position 395 to adenine with the KOD-Plus-Mutagenesis Kit (Toyobo). IDH1^{wt} or IDH1^{R132H} cDNA was inserted downstream of a CMV promoter in pIRES2-EGFP (Addgene). U87 human glioblastoma cells were transfected with Lipofectamine 2000 (Invitrogen). Transfection efficiency is about 40%. B: Western analysis. U87 cells were transfected with IDH1^{wt}, IDH1^{R132H}, or an empty-vector plasmid. Expressions of IDH1^{R132H} and IDH1^{wt} were confirmed by western blotting of cell lysates obtained 24 h after transfection. IDH1^{R132H} was specifically recognized with an anti-IDH1^{R132H} antibody. The upper arrow indicates the expression of IDH1 from the transfected plasmid and the lower one indicates endogenous IDH1 protein. IDH1: isocitrate dehydrogenase 1, NT: no transfection.

cells, and did not differ among plasmids transfected (Fig. 1A).

For siRNA experiments, U87 cells were transfected in the same way. siRNA oligonucleotides were synthesized by Sigma-Aldrich (Tokyo). The sequences of siRNA targeting SREBP1 were as follows:

5′-rCrGrGrArGrArArGrCUrGrCrCUrAUrArATT-3′ (sense) and
5′-UUrGrAUrArGrGrCrArGrCUUrCUUrCUUrCUrCrCrGTT-3′ (antisense).

The sequences of siRNA targeting SREBP2 were as follows:

5′-GUrGUrGrG3rAUUrGUrGUrCrCUrGrArGrCrGUTT-3′ (sense) and
5′-ArCrGrCUrCrArGrGrArCrArAUrCrArCrArCTT-3′ (antisense).

III. RNA micro array, quantitative reverse transcription-polymerase chain reaction (qRT-PCR)

Total RNA from transfected U87 cells was purified using the RNeasy Mini kit (Qiagen, Tokyo) according to the manufacturer's instructions. RNA microarray analysis was done by Filgen, Inc (Nagoya, Aichi). Total RNA was converted to cDNA with the SuperScript VILO cDNA synthesis kit (Invitrogen). Ten nanograms of cDNA was used as a template for quantitative PCR with gene-specific primers (Table 1) and SYBR green (Qiagen) by 40 cycles of denaturing at 95°C for 15 sec and annealing and extension at 60–62°C for 30 sec. These PCRs were repeated six times. The data were analyzed by the Student's *t*-test.

IV. Western blotting

Cells were lysed 24 h after transfection with a lysis buffer (1% sodium deoxycholate, 0.1% sodium dodecyl sulfate [SDS], 1% TritonX-100, 0.01 M Tris-HCl [pH 8.0], and 0.14 M NaCl) and protease inhibitors were incubated for 10 min on ice. Equal amounts of protein extracts were separated by SDS-polyacrylamide gel electrophoresis and then transferred to a polyvinylidene difluoride membrane. Membranes were blocked for 1h in Tris-buffered saline containing 0.1% Tween 20 and 5% nonfat milk and were then probed with anti-IDH1 (N-20) (sc-49996; Santa Cruz Biotechnology, Dallas, Texas, USA), anti-IDH1^{R132H} (DIA H09; Dianova, Warburgstr, Hamburg, Germany), anti-myc (R950-25; Invitrogen), anti-Retinoblastoma (Rb) (4H1) (#9309; Cell Signaling Technologies, Danvers, Massachusetts, USA), anti-phospho-Rb (Ser795) (#9301; Cell Signaling Technologies), or anti-β actin (C4) (sc-47778; Santa Cruz Biotechnology) antibodies. Membranes were then incubated with anti-mouse or anti-rabbit immunoglobulin G labeled with horseradish peroxidase. Chemiluminescent signals were detected on an imaging analyzer.

Table 1 Primer sequences and specific annealing temperatures used for quantitative PCR

Gene	Primer sequence	Annealing temperature (°C)
SREBP1	5′-AGGACAGCCTGGCTACCACA-3′	60
	5′-AGAAGCAGGTCACACAGGAACA-3′	
SREBP2	5′-CAAGGCCCTGGAAGTGACA-3′	60
	5′-AGGAACTCTGCTGCCCATCTG-3′	
SREBP 1a	5′-CTGCTGACCGACATCGAAGAC-3′	62
	5′-GATGCTCAGTGGCACTGACTCTTC-3′	
SREBP 1c	5′-CGGAGCCATGGATTGCACTTTC-3′	62
	5′-GATGCTCAGTGGCACTGACTCTCC-3′	
p53	5′-AGAGCTGAATGAGGCCTTGGAA-3′	60
	5′-GAGTCAGGCCCTTCTGTCTTGAAC-3′	
p21	5′-AAGACCATGTGGACCTGTCACTGT-3′	60
	5′-GAAGATCAGCCGGCGTTTG-3′	
MDM2	5′-TGGGCAGCTTGAAGCAGTTG-3′	60
	5′-CAGGCTGCCATGTGACCTAAGA-3′	
ACLY	5′-ATGCAGCAGCCAAGATGTTCA-3′	60
	5′-CACTCGCATGTCTGGGTTGTTTA-3′	
ACO2	5′-TTTGACAAGTGGGATGGCAAG-3′	60
	5′-CAATGAGCAGGTTGTTGGAGATG-3′	
IDH2	5′-GAGTGGAGCCATGACCAAGGA-3′	60
	5′-TGCTCTTGATGGTGTCGAGGA-3′	
IDH3A	5′-TTTACGCGAATGTCCGACCA-3′	60
	5′-TGATACTCTGCACGACTCCCATCAAC-3′	
MDH2	5′-TCTGAGCCACATCGAGAGACCAA-3′	60
	5′-GACTCCAGCCGGAATAACTACCAC-3′	
OGDH	5′-TGTCAATTCGATTCAAAGCTGGAG-3′	60
	5′-AAGGGTTGGCCACCAAGGA-3′	

SREBP1a and SREBP1c primers were synthesized by Sigma-Aldrich. The other primers were obtained from Takara Bio. ACLY: ATP citrate lyase, ACO2: mitochondrial aconitase 2, IDH: isocitrate dehydrogenase, MDH2: malate dehydrogenase 2, MDM2: murine double minute 2, OGDH: oxoglutarate dehydrogenase, PCR: polymerase chain reaction, SREBP: sterol regulatory element-binding protein.

V. ELISA

ELISA kits were used for the measurement of p21 (#7167; Cell Signaling Technologies) and p53 protein (CY-7049; CycLex, Ina, Nagano).

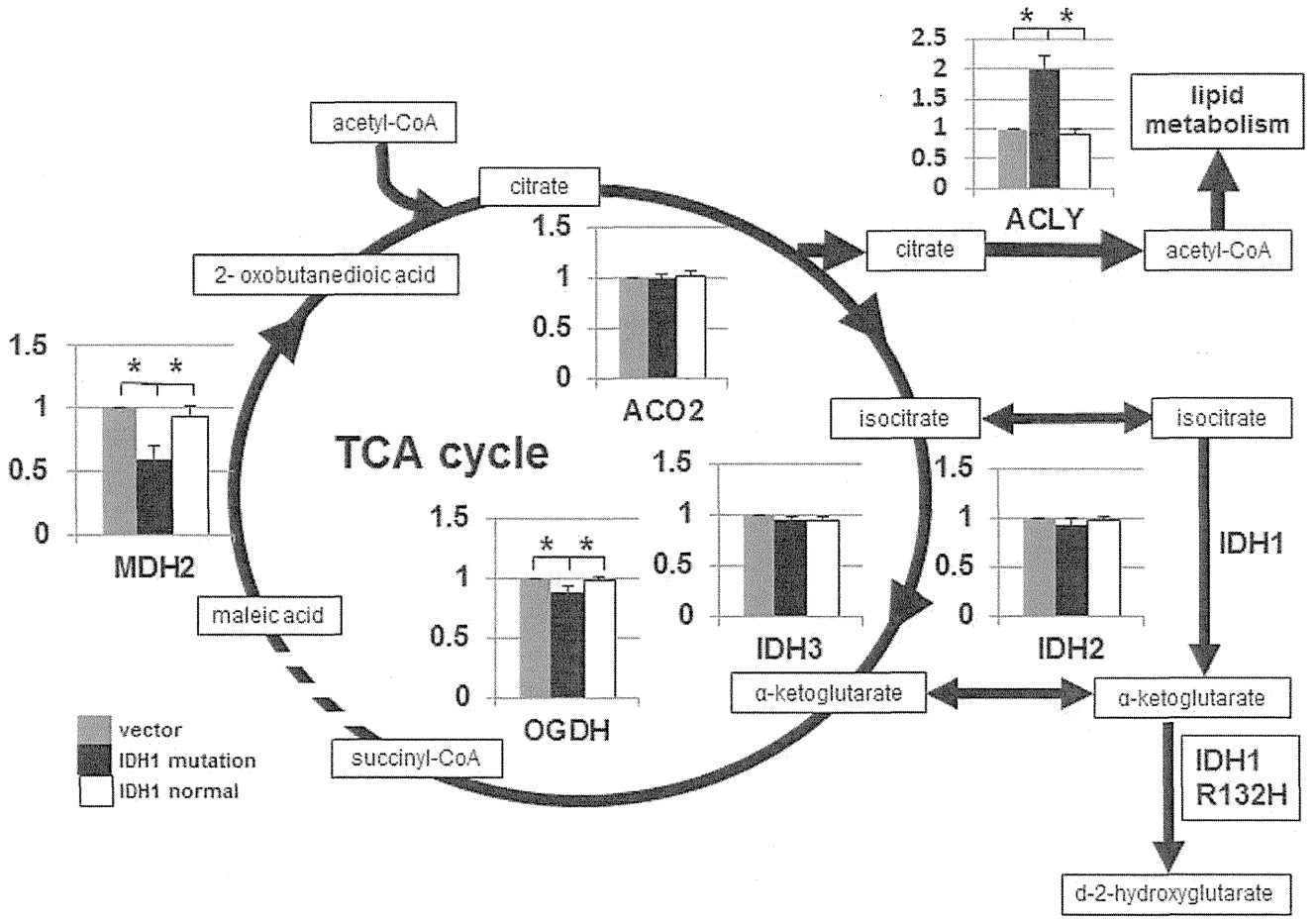

Fig. 2 Expression of IDH1^{R132H} alters metabolism in the TCA cycle in U87 human glioblastoma cells. The mRNA levels of enzymes involved in the TCA cycle were examined by quantitative reverse transcription-PCR. Notably, MDH2 mRNA levels were reduced in IDH1^{R132}-transfected cells while ACLY mRNA levels increased relative to IDH1^{wt}-transfected cells. ACLY: ATP citrate lyase, ACO2: mitochondrial aconitase 2, IDH1: isocitrate dehydrogenase 1, MDH2: malate dehydrogenase 2, OGDH: oxoglutarate dehydrogenase, PCR: polymerase chain reaction, TCA: tricarboxylic acid. *p < 0.05.

Results

I. U87 glioblastoma cells with IDH1^{R132H} altered the TCA cycle and lipid metabolism

A recent report showed that 2-HG increased specifically in IDH1-mutated gliomas and affected TCA cycle metabolism.[18] To examine the effect of the IDH1^{R132H} mutation on glioma cells, we constructed a plasmid expressing normal IDH1 or IDH1^{R132H} with a myc-tag (Fig. 1) and transfected them into U87 human glioblastoma cells. The result of qRT-PCR and RNA microarrays of IDH^{R132H}-transfected U87 cells relative to IDH^{WT}-transfected cells is summarized in Fig. 2 and Table 2. The expression levels of enzymes involved in the TCA cycle downstream of α-KG appeared lower in IDH1^{R132H}-transfected cells. In particular, an approximately 40% reduction in malate dehydrogenase 2 (MDH2) expression was detected relative to IDH^{WT}-transfected cells. However, the other TCA cycle enzymes upstream of α-KG were not affected by IDH1 mutation, probably due to relative depletion of α-KG in IDH1^{R132H}-transfected cells by competitive inhibition by 2-HG.[18] Interestingly, the level of ATP citrate lyase (ACLY) that converts citrate to acetyl-CoA in the cytoplasm significantly increased in IDH1^{R132H}-transfected cells, as revealed by RNA microarrays and qRT-PCR. Acetyl-CoA is then utilized for lipid synthesis as well. The other enzymes involved in lipid metabolism were up-regulated (Table 2). It is suggested that acetyl-CoA

Table 2 RNA microarray analysis of genes involved in TCA cycle and lipid metabolism

	TCA cycle		
	Genes	Accession number	Mutation/ normal*
ACO2	Aconitase 2, mitochondrial	NM_001098	1.01
IDH2	Isocitrate dehydrogenase 2 (NADP+)	NM_002168	1.14
IDH3	Isocitrate dehydrogenase 3 (NAD+)	NM_004135	0.98
OGDH	Oxoglutarate (alpha-ketoglutarate) dehydrogenase	NM_001003941	0.87
DLD	Dihydrolipoamide dehydrogenase	NM_000108	0.93
SUCLG	Succinate-CoA ligase	NM_001177599	0.92
SDH	Succinate dehydrogenase	NM_003000	0.94
MDH2	Malate dehydrogenase 2	NM_005918	0.84
ACLY	ATP citrate lyase	NM_001096	1.46
	Lipid metabolism		
SREBF1	Sterol regulatory element-binding transcription factor 1	NM_001005291	1.51
SREBF2	Sterol regulatory element-binding transcription factor 2	NM_004599	1.35
SCAP	SREBF chaperone	NM_012235	1.57
FASN	Fatty acid synthase	NM_004104	2.06
ACACA	Acetyl-CoA carboxylase alpha	NM_198834	1.43
ACACB	Acetyl-CoA carboxylase beta	NM_001093	2.51
HMGCR	3-Hydroxy-3-methylglutaryl-CoA reductase	NM_000859	2.03

*The ratio of the amount of mRNA in IDH1-mutation-expressing cells to IDH1-normal cells. IDH1: isocitrate dehydrogenase 1, mRNA: messenger ribonucleic acid, TCA: tricarboxylic acid.

is preferentially metabolized for lipid synthesis rather than in the TCA cycle in IDH^{R132H} U87 cells.

II. Up-regulation of p21 depends on SREBP1a

Increases in the expression levels of SREBP1 and -2 prompted us to examine p21, a cyclin-dependent kinase inhibitor. p21, which halts the cell cycle at G1, is regulated by SREBP.[12] qRT-PCR analysis showed that IDH1^{R132H}-transfected cells up-regulated SREBP1a, 1c, and 2 (Fig. 3A, B). In particular, SREBP1a has been shown to activate p21 expression and leads to cell growth arrest.[12] In order to investigate the relationship between p21 and SREBP1 in U87 cells, we performed siRNA experiments. siRNA for SREBP1 specifically knocked down SREBP1a and 1c and siRNA for SREBP2 suppressed its target mRNA (Fig. 3C). Knock-down of SREBP1, but not SREBP2, specifically induced a decrease in p21 expression in IDH^{R132H}-transfected cells (Fig. 3D). These results indicated that the R132H mutation in IDH1 induced the expression of SREBPs and that SREBP1 enhanced the expression of p21 in IDH1^{R132H}-transfected cells.

III. IDH^{R132H} up-regulates p21 independent of p53

p53, a tumor suppressor, regulates p21 expression and is negatively regulated by murine double minute 2 (MDM2).[5] To examine the effect of IDH1^{R132H} on the p53–p21 signaling pathway, we measured p21, p53, and MDM2 mRNA levels in IDH1^{wt}- and IDH1^{R132H}-transfected cells by qRT-PCR and assayed p21 and p53 by ELISA (Fig. 4, Table 3). p21 was up-regulated in IDH1^{R132H}-transfected cells. However, p53 and MDM2 mRNA levels did not differ among the three groups (Fig. 4). These results suggested that the up-regulation of p21 protein was mediated by direct activation by SREBP, but not by p53.

p21 protein inhibits the phosphorylation of Rb protein, one of the tumor suppressors. Nonphosphorylated Rb protein binds E2F transcription factor and prevents E2F from activating gene expression. Phosphorylated Rb fails to bind E2F and permits cells entering from the G1 phase to the S phase in the cell cycle.[4] Western blot analysis of Rb protein indicated that the level of the phosphorylated form, relative to total Rb protein, decreased in IDH1^{R132H}-transfected cells (Fig. 5A), suggesting slowing in progression of the cell cycle in IDH1-mutated U87

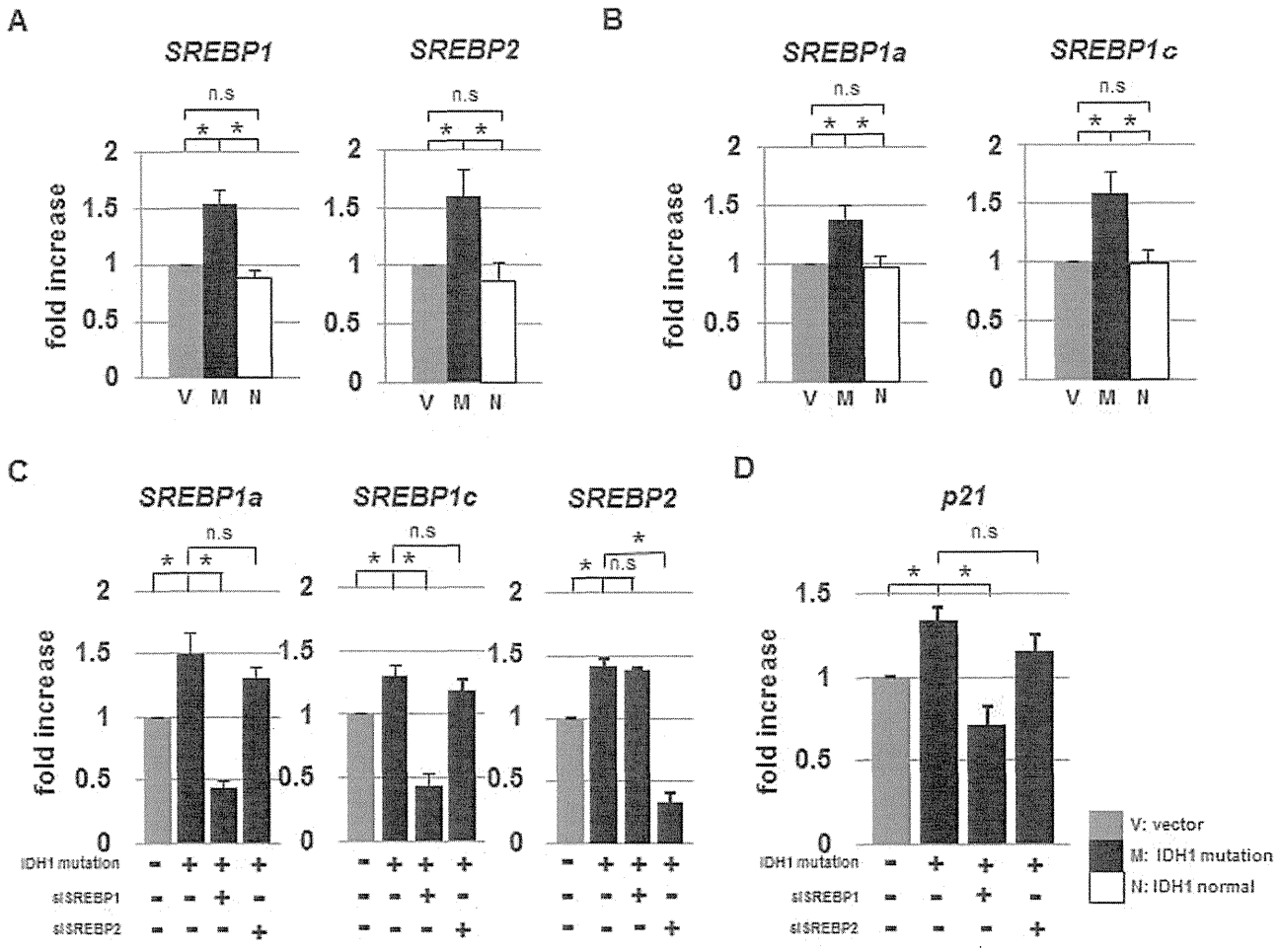

Fig. 3 The SREBP family of transcription factors were up-regulated in IDH1^{R132H}-transfected U87 cells. Quantitative reverse transcription-PCR analysis of SREBP1 and 2 (A), and SREBP1a and SREBP1c (B) mRNA levels increased in IDH1^{R132H}-U87 cells. C: siRNA for SREBP1 and 2 used in the present study specifically suppressed its target mRNA. D: p21 mRNA levels that increased in IDH1^{R132H}-U87 cells were suppressed by knock-down of SREBP1, not SREBP2. IDH1: isocitrate dehydrogenase 1, M: IDH1^{R132H} transfection, N: IDH1^{wt} transfection, n.s: not significant, PCR: polymerase chain reaction, SREBP: sterol regulatory element-binding protein, V: empty vector. *$p < 0.05$.

cells (Fig. 5B).

Discussion

Since gliomas invasively grow into normal brain tissue and is thus difficult to surgically resect completely, the therapeutic outcome of gliomas was extremely poor. Although improved surgical techniques in combination with an alkylating agent temozolomide have made the median survival time of glioblastomas longer (21.4 months),[15] the outcomes of glioblastomas are still poor relative to other carcinomas. However, gliomas bearing the IDH1 mutation are associated with better outcomes.[16,24]

The mutated IDH1 produces 2-HG from α-KG in the cytoplasm.[6] 2-HG competitively inhibits α-keto acid transaminase, thereby suppressing the TCA cycle.[18] The present analyses confirmed that the TCA cycle was down-regulated in IDH1^{R132H}-cells (Fig. 2), which has been proposed as the Warburg effect.[11,13,22,24,25] Furthermore, it has been said that this down-regulation is associated with a selective advantage for cancer cells because nutrients are converted to building blocks such as lipids to be used for proliferation rather than being oxidized in the TCA cycle.[18] The present study showed that down-regulation of the TCA cycle and up-regulation of ACLY, which converts citrate in the cytoplasm

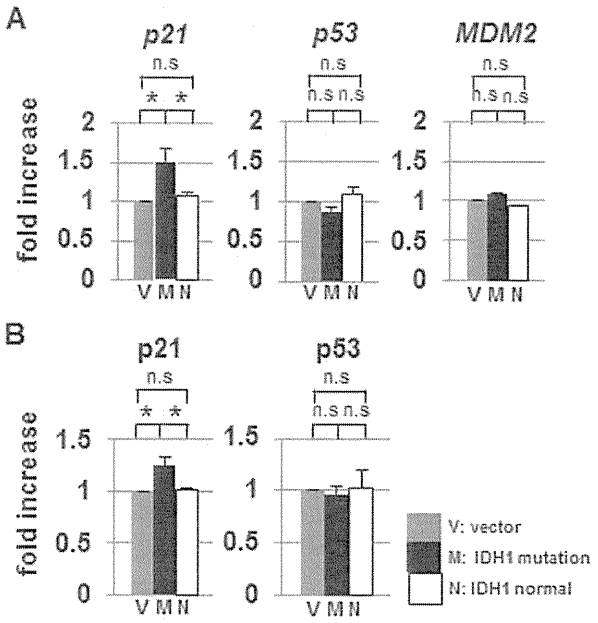

Fig. 4 p21 was specifically up-regulated in IDH1^{R132H}-expressing U87 cells. A: Quantitative reverse transcription-PCR analysis of p21, p53, and MDM2 mRNA levels in IDH1^{wt}- and IDH1^{R132H}-transfectedU87 cells. p21 mRNA was significantly increased in IDH1^{R132H} cells. However, p53 and its negative regulator MDM2 mRNA levels did not show significant changes, relative to IDH^{wt}-transfected cells. B: ELISA of p21 and p53. p21 significantly increased in IDH1^{R132H}-expressing U87 cells. IDH: isocitrate dehydrogenase, M: IDH1^{R132H} transfection, MDM2: murine double minute 2, N: IDH1^{wt} transfection, n.s: not significant, PCR: polymerase chain reaction, V: empty vector. *$p < 0.05$.

Table 3 Representative genes associated with cell cycle progression in IDH1-mutation-expressing cells

Genes	Accession number	Mutation/normal*
MDM2	NM_002392	1.03
p15	NM_004936	1.47
p16	NM_000077	1.37
p18	NM_001262	1.03
p19	NM_001800	1.35
p21	NM_000389	1.50
p27	NM_004064	1.22
p45	NM_005983	2.03
CDK2	NM_001798	0.95
CDK4	NM_000075	0.85
CDK6	NM_00114530	1.07
CDC6	NM_001254	1.16
Cyclin A1	NM_001111045	0.98
Cyclin A2	NM_001237	1.13
Cyclin B1	NM_031966	0.80
Cyclin B2	NM_004701	0.75
Cyclin B3	NM_033031	1.19
Cyclin D3	NM_001136017	0.85
Cyclin E1	NM_001238	0.98
Cyclin E2	NM_057749	0.78
E2F1	NM_005225	1.12
E2F3	NM_001949	1.17
E2F4	NM_001950	1.00
E2F5	NM_001083588	0.92
E2F6	NM_198256	0.82
E2F8	NM_024680	1.28

*The ratio of the amount of mRNA in IDH1-mutation-expressing cells relative to IDH1-normal cells. CDC6: cell division cycle 6, CDK: cyclin-dependent kinase, IDH1: isocitrate dehydrogenase 1, MDM2: murine double minute 2, mRNA: messenger ribonucleic acid.

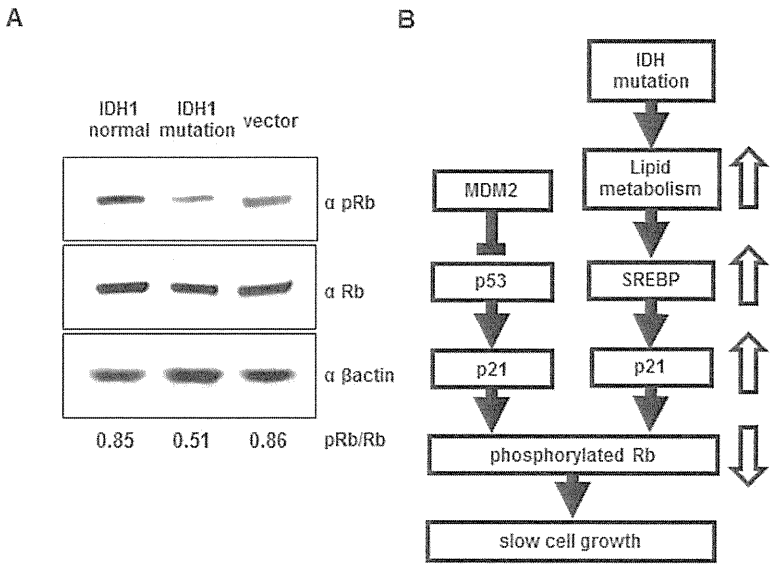

Fig. 5 A: Rb protein in IDH1^{R132H}-U87 cells. Cells were lysed 24 h after transfection with IDH1^{wt}, IDH1^{R132H}, and a vector plasmid. Western analysis of pRb and total Rb shows that pRb decreased in IDHR^{132H}-transfected cells. For comparison, the intensity of each band was measured and the ratio of pRb to Rb (pRb/Rb) was calculated as shown at the bottom. B: A proposed signaling cascade leading to nonaggressive cancer associated with the IDH1 mutation. IDH1: isocitrate dehydrogenase 1, pRb: phosphorylated Rb, Rb: retinoblastoma.

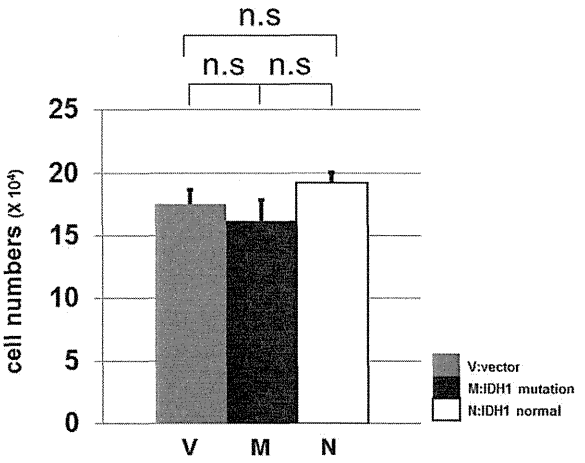

Fig. 6 The comparison of growth of U87 cells after transfection. 1 × 10^4 cells of U87 were transfected with $IDH1^{R132H}$ (M), $IDH1^{wt}$ (N), or a vector plasmid (V). Three days after transfection, we counted the number of cells. The experiment was performed in triplicate. The U87 cells transfected with IDH1 mutation plasmid were less proliferative compared to those transfected with IDH1 normal or a vector plasmid although the difference was not statistically significant. IDH1: isocitrate dehydrogenase 1, n.s: not significant.

into acetyl-CoA, resulted in enhanced lipid metabolism (Fig. 2, Table 2). The R132H mutation in IDH1 induced shunting of carbons from glycolysis into *de novo* synthesis of lipid rather than into the TCA cycle. The enhanced lipid metabolism by the mutated IDH1can be relevant to increased SREBP expression.

The transcription factor to regulate lipid synthesis from acetyl-CoA in the cytoplasm is SREBP. Our data clearly showed that $IDH1^{R132H}$ induced increases in the mRNA levels of all SREBP family transcripts, 1a, 1c, and 2 (Fig. 4). SREBP1a and 2 have been shown to enhance p21 promoter activity,[12] which was also confirmed in U87glioblastoma cells by qRT-PCR and siRNA knock-down experiments (Fig. 3C, D). Another pathway that regulates p21 is the p53-MDM2 cascade. As shown in Fig. 4, p53 and its mRNA levels in $IDH1^{R132H}$-transfected cells did not differ from IDH^{wt}-transfected cells, which supported that p21 was up-regulated via the SREBP pathway independent of the p53 pathway (Fig. 4). In addition, it has been reported that glycolysis is enhanced in glioma with the IDH1 mutation,[18] and that glycolysis suppresses p53.[14] This line of evidence supports p53 not playing a role in p21 activation in $IDH1^{R132H}$ U87 cells. Recently, $IDH1^{R132H}$ has been reported to be associated with SREBP1a activation and cellular proliferation.[28] However, the precise mechanism how $IDH1^{R132H}$ induces SREBP1a activation was not revealed. Although $IDH1^{R132H}$ is associated with slow tumor progression, it is controversial whether $IDH1^{R132H}$ mutation induces or suppresses cell growth in cultured glioma cells. Another study reported that stably $IDH1^{R132H}$ expressing U87 cells decreased cellular proliferation.[2]

In an attempt to demonstrate the direct association between the $IDH1^{R132H}$ and the retardation of cell growth, we analyzed the cell cycle profile of the transfected U87 cells. Unfortunately, we failed to get reproducible data, probably due to a subtle difference between $IDH1^{wt}$- and $IDH1^{R132H}$-cells (data not shown). We next measured the proliferation rate of $IDH1^{wt}$- and $IDH1^{R132H}$-transfected cells. Although the difference was not statistically significant, the U87 cells transfected with $IDH1^{R132H}$ plasmid tended to slower growth (Fig. 6). Accumulation of subtle growth retardation after a number of cell division in $IDH1^{R132H}$ glioma may lead to smaller tumor burden. The results obtained in the present study is based on the experiments with the U87 glioblastoma cell line, one of the widely employed in cultured brain tumor cells. However, it is desirable to examine other brain tumor cell lines and patients' glioblastomas in order to confirm the present results.

Several reports implicate doxidative stress[1,6,8,17,25] or methylation of the MGMT promoter portion in gliomas with the IDH1 mutation[3,19] important for a nonaggressive profile. We propose that suppression of the TCA cycle and subsequent enhancements in lipid metabolism induce up-regulation of the SREBP family, which results in the increased activity of p21 and decrease in phosphorylation of Rb protein (Fig. 5B). The R132H mutation in IDH1 appears to give rise to diverse metabolic changes, such as increased oxidative stress, inhibition of the TCA cycle, and enhanced lipid metabolism. The sum of all these alterations may make tumor cells nonaggressive. More detailed analysis of the metabolic changes induced by the IDH1 mutation will help us understand the mechanism of the low-grade malignant profile of an $IDH1^{R132H}$ glioma.

Acknowledgments

Satsuki Miyata received a Research Award to JMU graduate students. Metabolome analysis was supported by Human Metabolome Technologies, Inc.

Conflicts of Interest Disclosure

The authors declare no conflicts of interest.

References

1) Bleeker FE, Atai NA, Lamba S, Jonker A, Rijkeboer D, Bosch KS, Tigchelaar W, Troost D, Vandertop WP, Bardelli A, Van Noorden CJ: The prognostic IDH1(R132) mutation is associated with reduced NADP+-dependent IDH activity in glioblastoma. *Acta Neuropathol* 119: 487–494, 2010
2) Bralten LB, Kloosterhof NK, Balvers R, Sacchetti A, Lapre L, Lamfers M, Leenstra S, de Jonge H, Kros JM, Jansen EE, Struys EA, Jakobs C, Salomons GS, Diks SH, Peppelenbosch M, Kremer A, Hoogenraad CC, Smitt PA, French PJ: IDH1 R132H decreases proliferation of glioma cell lines in vitro and in vivo. *Ann Neurol* 69: 455–463, 2011
3) Christensen BC, Smith AA, Zheng S, Koestler DC, Houseman EA, Marsit CJ, Wiemels JL, Nelson HH, Karagas MR, Wrensch MR, Kelsey KT, Wiencke JK: DNA methylation, isocitrate dehydrogenase mutation, and survival in glioma. *J Natl Cancer Inst* 103: 143–153, 2011
4) Cmielová J, Rezáčová M: p21Cip1/Waf1 protein and its function based on a subcellular localization. *J Cell Biochem* 112: 3502–3506, 2011
5) Colman MS, Afshari CA, Barrett JC: Regulation of p53 stability and activity in response to genotoxic stress. *Mutat Res* 462: 179–188, 2000
6) Dang L, White DW, Gross S, Bennett BD, Bittinger MA, Driggers EM, Fantin VR, Jang HG, Jin S, Keenan MC, Marks KM, Prins RM, Ward PS, Yen KE, Liau LM, Rabinowitz JD, Cantley LC, Thompson CB, Vander Heiden MG, Su SM: Cancer-associated IDH1 mutations produce 2-hydroxyglutarate. *Nature* 462: 739–744, 2009
7) Edwards PA, Tabor D, Kast HR, Venkateswaran A: Regulation of gene expression by SREBP and SCAP. *Biochim Biophys Acta* 1529: 103–113, 2000
8) Fu Y, Huang R, Du J, Yang R, An N, Liang A: Glioma-derived mutations in IDH: from mechanism to potential therapy. *Biochem Biophys Res Commun* 397: 127–130, 2010
9) Fu Y, Huang R, Zheng Y, Zhang Z, Liang A: Glioma-derived mutations in isocitrate dehydrogenase 2 beneficial to traditional chemotherapy. *Biochem Biophys Res Commun* 410: 218–223, 2011
10) Gross S, Cairns RA, Minden MD, Driggers EM, Bittinger MA, Jang HG, Sasaki M, Jin S, Schenkein DP, Su SM, Dang L, Fantin VR, Mak TW: Cancer-associated metabolite 2-hydroxyglutarate accumulates in acute myelogenous leukemia with isocitrate dehydrogenase 1 and 2 mutations. *J Exp Med* 207: 339–344, 2010
11) Hsu PP, Sabatini DM: Cancer cell metabolism: Warburg and beyond. *Cell* 134: 703–707, 2008
12) Inoue N, Shimano H, Nakakuki M, Matsuzaka T, Nakagawa Y, Yamamoto T, Sato R, Takahashi A, Sone H, Yahagi N, Suzuki H, Toyoshima H, Yamada N: Lipid synthetic transcription factor SREBP-1a activates p21WAF1/CIP1, a universal cyclin-dependent kinase inhibitor. *Mol Cell Biol* 25: 8938–8947, 2005
13) Kondoh H: Cellular life span and the Warburg effect. *Exp Cell Res* 314: 1923–1928, 2008
14) Mason EF, Zhao Y, Goraksha-Hicks P, Coloff JL, Gannon H, Jones SN, Rathmell JC: Aerobic glycolysis suppresses p53 activity to provide selective protection from apoptosis upon loss of growth signals or inhibition of BCR-Abl. *Cancer Res* 70: 8066–8076, 2010
15) Muragaki Y, Maruyama T, Iseki H, Tanaka M, Shinohara C, Takakura K, Tsuboi K, Yamamoto T, Matsumura A, Matsutani M, Karasawa K, Shimada K, Yamaguchi N, Nakazato Y, Sato K, Uemae Y, Ohno T, Okada Y, Hori T: Phase I/IIa trial of autologous formalin-fixed tumor vaccine concomitant with fractionated radiotherapy for newly diagnosed glioblastoma. Clinical article. *J Neurosurg* 115: 248–255, 2011
16) Parsons DW, Jones S, Zhang X, Lin JC, Leary RJ, Angenendt P, Mankoo P, Carter H, Siu IM, Gallia GL, Olivi A, McLendon R, Rasheed BA, Keir S, Nikolskaya T, Nikolsky Y, Busam DA, Tekleab H, Diaz LA, Hartigan J, Smith DR, Strausberg RL, Marie SK,Shinjo SM, Yan H, Riggins GJ, Bigner DD, Karchin R, Papadopoulos N, Parmigiani G, Vogelstein B, Velculescu VE, Kinzler KW: An integrated genomic analysis of human glioblastoma multiforme. *Science* 321: 1807–1812, 2008
17) Reitman ZJ, Yan H: Isocitrate dehydrogenase 1 and 2 mutations in cancer: alterations at a crossroads of cellular metabolism. *J Natl Cancer Inst* 102: 932–941, 2010
18) Reitman ZJ, Jin G, Karoly ED, Spasojevic I, Yang J, Kinzler KW, He Y, Bigner DD, Vogelstein B, Yan H: Profiling the effects of isocitrate dehydrogenase 1 and 2 mutations on the cellular metabolome. *Proc Natl Acad Sci U S A* 108: 3270–3275, 2011
19) Sanson M, Marie Y, Paris S, Idbaih A, Laffaire J, Ducray F, El Hallani S, Boisselier B, Mokhtari K, Hoang-Xuan K, Delattre JY: Isocitrate dehydrogenase 1 codon 132 mutation is an important prognostic biomarker in gliomas. *J Clin Oncol* 27: 4150–4154, 2009
20) Shimano H, Horton JD, Shimomura I, Hammer RE, Brown MS, Goldstein JL: Isoform 1c of sterol regulatory element binding protein is less active than isoform 1a in livers of transgenic mice and in cultured cells. *J Clin Invest* 99: 846–854, 1997
21) Stupp R, Mason WP, van den Bent MJ, Weller M, Fisher B, Taphoorn MJ, Belanger K, Brandes AA, Marosi C, Bogdahn U, Curschmann J, Janzer RC, Ludwin SK, Gorlia T, Allgeier A, Lacombe D, Cairncross JG, Eisenhauer E, Mirimanoff RO: Radiotherapy plus concomitant and adjuvant temozolomide for glioblastoma. *N Engl J Med* 352: 987–996, 2005
22) Vander Heiden MG, Cantley LC, Thompson CB: Understanding the Warburg effect: the metabolic requirements of cell proliferation. *Science* 324: 1029–1033, 2009
23) Van Meir EG, Kikuchi T, Tada M, Li H, Diserens AC, Wojcik BE, Huang HJ, Friedmann T, de Tribolet N, Cavenee WK: Analysis of the p53 gene and its expression in human glioblastoma cells. *Cancer Res* 54: 649–652, 1994